

# 1 Characterizing the Discoloration of Methylene Blue in Fe<sup>0</sup>/H<sub>2</sub>O Systems.

2 C. Noubactep

3 Angewandte Geologie, Universität Göttingen, Goldschmidtstraße 3, D - 37077 Göttingen, Germany.

4 Tel.: +49 551 39 3191, Fax.: +49 551 399379, e-mail: cnoubac@gwdg.de

## 6 Abstract

7 Methylene blue (MB) was used as a model molecule to characterize the aqueous reactivity of  
8 metallic iron in Fe<sup>0</sup>/H<sub>2</sub>O systems. Likely discoloration mechanisms under used experimental  
9 conditions are: (i) adsorption onto Fe<sup>0</sup> and Fe<sup>0</sup> corrosion products (CP), (ii) co-precipitation with  
10 in-situ generated iron CP, (iii) reduction to colorless leukomethylene blue (LMB). MB  
11 mineralization (oxidation to CO<sub>2</sub>) is not expected. The kinetics of MB discoloration by Fe<sup>0</sup>,  
12 Fe<sub>2</sub>O<sub>3</sub>, Fe<sub>3</sub>O<sub>4</sub>, MnO<sub>2</sub>, and granular activated carbon were investigated in assay tubes under  
13 mechanically non-disturbed conditions. The evolution of MB discoloration was monitored  
14 spectrophotometrically. The effect of availability of CP, Fe<sup>0</sup> source, shaking rate, initial pH  
15 value, and chemical properties of the solution were studied. The results present evidence  
16 supporting co-precipitation of MB with in-situ generated iron CP as main discoloration  
17 mechanism. Under high shaking intensities (> 150 min<sup>-1</sup>), increased CP generation yields a  
18 brownish solution which disturbed MB determination, showing that a too high shear stress  
19 induced the suspension of in-situ generated corrosion products. The present study clearly  
20 demonstrates that comparing results from various sources is difficult even when the results are  
21 achieved under seemingly similar conditions. The appeal for an unified experimental procedure  
22 for the investigation of processes in Fe<sup>0</sup>/H<sub>2</sub>O systems is reiterated.

24 **Keywords:** Adsorption; Co-precipitation; Iron Corrosion, Methylene Blue; Zerovalent Iron.

## 25 **Introduction**

26 Permeable reactive barriers using elemental iron -based alloys ( $\text{Fe}^0$ -based alloys widely termed as  
27 zerovalent iron) as a reactive medium have been proven to be an efficient and affordable  
28 technology for removing inorganics and organics species from groundwater [1 -7]. Even living  
29 species like viruses have been successfully removed [8]. Despite 15 years of intensive  
30 investigations, the removal mechanisms of contaminants in  $\text{Fe}^0$  treatment systems are still not  
31 well understood [9,10]. In fact, the well -established premise that contaminant removal results  
32 from the low electrode potential of the redox couple  $\text{Fe}^{\text{II}}/\text{Fe}^0$  ( $E^0 = -0.44 \text{ V}$ ) can not explain why  
33 redox-insensitive species are quantitatively removed [11,12]. However, understanding the nature  
34 of primary processes yielding to contaminant removal in  $\text{Fe}^0/\text{H}_2\text{O}$  systems is of fundamental  
35 importance for advancing technological applications. The accurate knowledge of these processes  
36 will favor the identification of factors dominating the general reactivity of  $\text{Fe}^0/\text{H}_2\text{O}$  systems,  
37 which is of fundamental importance for the long -term stability of iron reactive barriers. A more  
38 rational devising of  $\text{Fe}^0$  treatment systems for an effective and economical contaminant removal  
39 could be achieved.

40  $\text{Fe}^0$  oxidation releases dissolved iron species ( $\text{Fe}^{\text{II}}$ ,  $\text{Fe}^{\text{III}}$ ) which hydrolyse with increasing pH and  
41 precipitate primarily as hydrous oxides (oxide-film) or corrosion products (CP). Oxide-films (CP)  
42 of varied composition and thickness develop at all aqueous  $\text{Fe}^0/\text{H}_2\text{O}$  interfaces [13,14].  
43 Therefore, an aqueous  $\text{Fe}^0$  treatment system ( $\text{Fe}^0/\text{H}_2\text{O}$  system) is made up of  $\text{Fe}^0$ , iron oxides  
44 (oxide-film), and water ( $\text{H}_2\text{O}$ ). Contaminant adsorption onto the oxide -film and reduction by  $\text{Fe}^0$   
45 have mostly been evaluated as separate, independent processes that occur simultaneously or  
46 sequentially on metal surfaces. However, contaminants may be primarily quantitatively  
47 sequestered by in situ generated hydrous iron oxides (co -precipitation) [11,12]. Initial corrosion  
48 products polymerise and precipitate, first as very reactive oxides having short -range crystalline

49 order and after aging as crystalline oxides [15 -18]. Subsequent abiotic direct reduction (electrons  
50 are transferred from Fe<sup>0</sup>) or indirect reduction (electrons from Fe<sup>II</sup>, H/H<sub>2</sub>) of adsorbed or co -  
51 precipitated contaminants is possible. As a rule co -precipitation occurs whenever the  
52 precipitation of a major species (e.g., iron oxide) takes place in the presence of foreign species  
53 (e.g., contaminants) and has been documented for organ ics [16,17,19,20], inorganics [21 -23] and  
54 living species [8] under various conditions. Generally, adsorption and co -precipitation are  
55 considered to be related such that in order for co -precipitation to occur, sorption to the surface of  
56 a forming solid occu rs and the adsorbed species is then sequestered in the matrix of the  
57 precipitating phase (e.g. iron hydroxide). However, co -precipitation in Fe<sup>0</sup>/H<sub>2</sub>O systems may be  
58 primarily regarded as a non -specific removal mechanism [11,17] as to be demonstrated in this  
59 study of a process involving the discoloration of methylene blue.

60 Methylene blue (MB) is a well-known redox indicator [24] and is a cationic thiazine dye with the  
61 chemical name tetramethylthionine chloride. It has a characteristic deep blue colour in the  
62 oxidized state; the reduced form (leukomethylene blue - LMB) is colorless. MB has been widely  
63 used in environmental sciences primarily to assess the suitability of various materials for  
64 wastewater discoloration [25-29]. The mechanism of MB removal by Fe<sup>0</sup>-based materials which  
65 may be suitable for environmental remediation (cast iron, low alloy steel) has not been yet  
66 systematically investigated. Imamura et al. [30] investigated the mechanism of adsorption of  
67 methylene blue and its congeners onto stainless st eel particles. MB has also been used for  
68 corrosion inhibition of mild steel in acid solutions [31].

69 The literature on “Fe<sup>0</sup> technology” is characterized by the fact that, since the effectiveness of Fe<sup>0</sup>  
70 reactive walls to degrade solvents was demonstrated, the feasibility of applying Fe<sup>0</sup> to treat other  
71 compounds (or group of compounds) are performed without previous systematic investigations  
72 [9]. For example, while presenting the discoloration of MB by a Fe/Cu bimetallic system, Ma et

73 al. [28] referenced several works dealing with dyes in general [32 -34]. The authors did not  
74 specified whether the referenced works have used MB. Furthermore, their experimental  
75 procedure did not include a system with  $\text{Fe}^0$  alone to evidence the improvement induced by  $\text{Cu}^0$   
76 addition.

77 Given the diversity of contaminant removal mechanisms in a  $\text{Fe}^0/\text{H}_2\text{O}$  system, an approach to  
78 elucidate the mechanism of contaminant removal in the system is to characterise the removal  
79 process of the contaminant in question by a pure adsorbent (e.g. activated carbon - AC), and  
80 model iron corrosion products ( $\text{Fe}_2\text{O}_3$ ,  $\text{Fe}_3\text{O}_4$ ) under the same experimental conditions [35]. Here,  
81 comparing the evolution of contaminant removal in the systems with pure adsorption (AC,  $\text{Fe}_2\text{O}_3$ ,  
82  $\text{Fe}_3\text{O}_4$ ) and in the system with  $\text{Fe}^0$  will help discussing the removal mechanism. Another  
83 approach consists in introducing  $\text{MnO}_2$  to delay the availability of corrosion products in the  
84 system [36].  $\text{MnO}_2$  readily reacts with  $\text{Fe}^{\text{II}}$  from  $\text{Fe}^0$  corrosion products: reductive dissolution of  
85  $\text{MnO}_2$  by  $\text{Fe}^{\text{II}}$  [37]. If the process of contaminant removal is coupled with the precipitation of  
86 iron, then contaminant removal will be delayed as long as the added amount of  $\text{MnO}_2$  consumes  
87  $\text{Fe}^{\text{II}}$  for reductive dissolution as it will be presented later.

88 The present study is an attempt to elucidate the physico-chemical mechanism of MB  
89 discoloration in  $\text{Fe}^0/\text{H}_2\text{O}$  systems by comparing the kinetics and/or the extent of MB  
90 discoloration by  $\text{Fe}^0$  and different materials: granular activated carbon (GAC or AC), iron oxides  
91 ( $\text{Fe}_2\text{O}_3$ ,  $\text{Fe}_3\text{O}_4$ ) and manganese dioxide ( $\text{MnO}_2$ ). Non-disturbed (not shaken or shaking at  $0 \text{ min}^{-1}$ )  
92 batch experiments were performed in order to allow formation and transformation of corrosion  
93 products at the surface of  $\text{Fe}^0$  as it occurs in the nature and in column experiments. The effects of  
94 various factors (initial pH value, mixing intensity, particle size,  $\text{Fe}^0$  source,  $\text{Cl}^-$ ,  $\text{HCO}_3^-$ , EDTA)  
95 on the extent of MB discoloration are discussed. The results show that MB quantitative

96 discoloration is mostly due to co-precipitation with in-situ generated corrosion products.

97 Therefore, MB discoloration occurs within the oxide-film on Fe<sup>0</sup>.

## 98 **Background of the Experimental Methodology**

99 A survey of the electrode potentials of the redox couples relevant for the discussion in this study

100 [Fe<sup>II</sup><sub>(aq)</sub>/Fe<sup>0</sup>, Fe<sup>III</sup><sub>(aq)</sub>/Fe<sup>II</sup><sub>(aq)</sub>, Fe<sup>III</sup><sub>(s)</sub>/Fe<sup>II</sup><sub>(s)</sub>, MnO<sub>2</sub>/Mn<sup>2+</sup>, O<sub>2</sub>/HO<sup>-</sup>, and MB<sup>+</sup>/LMB (Eq. 1 to Eq. 6)]

101 suggests that from the available iron species, Fe<sup>0</sup> and Fe<sup>II</sup><sub>(s)</sub> can reduce MB. Equation 2 is that of

102 the adsorbed Fe<sup>II</sup> known as structural Fe<sup>II</sup>. The electrode potential of this redox couple was

103 determined by White and Patterson [38]. The electrode potential of Eq. 3 to 6 shows that Fe<sup>III</sup><sub>(aq)</sub>,

104 dissolved O<sub>2</sub> and MnO<sub>2</sub> may re-oxidize colorless LMB to blue MB<sup>+</sup>.

	Reaction	E <sup>0</sup> (V)	Eq.
	Fe <sup>2+</sup> + 2 e <sup>-</sup> ⇌ Fe <sup>0</sup>	-0.44	(1)
	Fe <sup>3+</sup> <sub>(s)</sub> + e <sup>-</sup> ⇌ Fe <sup>2+</sup> <sub>(s)</sub>	-0.36 to -0.65	(2)
	MB <sup>+</sup> + 2 e <sup>-</sup> + H <sup>+</sup> ⇌ LMB	0.01	(3)
	Fe <sup>3+</sup> <sub>(aq)</sub> + e <sup>-</sup> ⇌ Fe <sup>2+</sup> <sub>(aq)</sub>	0.77	(4)
	O <sub>2(aq)</sub> + 2 H <sub>2</sub> O + 4 e <sup>-</sup> ⇌ 4 OH <sup>-</sup>	0.81	(5)
	MnO <sub>2</sub> + 4 H <sup>+</sup> + 2 e <sup>-</sup> ⇌ Mn <sup>2+</sup> <sub>(aq)</sub> + 2 H <sub>2</sub> O	1.23	(6)

105 Reductive MB discoloration in this study may be the result of either (i) Fe<sup>0</sup> corrosion (oxidation

106 to Fe<sup>II</sup><sub>(aq)</sub>) (Eq. 1) or (ii) oxidation of adsorbed Fe<sup>II</sup> (Fe<sup>II</sup><sub>(s)</sub> to Fe<sup>III</sup><sub>(s)</sub> - Eq. 2). Additionally, MB

107 adsorption onto in situ generated and aged Fe<sup>0</sup> corrosion products and MB entrapment in the

108 structure of forming corrosion products (co-precipitation) are two further discoloration

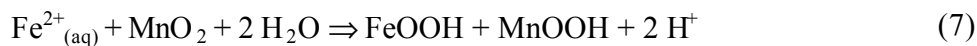
109 mechanisms. Therefore, it is difficult to resolve the effect of specific redox reactions on MB

110 discoloration from the effects of other processes. To resolve this problem two additives are added

111 to Fe<sup>0</sup>: granular activated carbon (GAC) and manganese dioxide (MnO<sub>2</sub>). GAC is a pure

112 adsorbent for MB [25] whereas reductive dissolution of MnO<sub>2</sub> has been reported to decolorize

113 MB [39]. The presentation above shows that  $\text{MnO}_2$  should re-oxidise reduced LMB (no  
 114 discoloration). The refore, MB discoloration in the presence of  $\text{MnO}_2$  could only result from  
 115 adsorption. On the other hand,  $\text{MnO}_2$  is known to be reductively dissolved by  $\text{Fe}^{\text{II}}$  [37, 40]. By  
 116 consuming  $\text{Fe}^{\text{II}}$ ,  $\text{MnO}_2$  accelerates  $\text{Fe}^0$  corrosion, producing more adsorption or co-precipitation  
 117 agents for MB. Increased adsorption is supported by the fact that iron corrosion products are of  
 118 higher specific surface area ( $> 40 \text{ m}^2 \text{ g}^{-1}$ ) than the used  $\text{Fe}^0$  ( $0.29 \text{ m}^2 \text{ g}^{-1}$ ). The reductive  
 119 dissolution of  $\text{MnO}_2$  (Eq. 7 and 8) produce further new reactive adsorbents ( $\text{MnOOH}$  and  
 120  $\text{FeOOH}$ ).



121 Noubactep et al. [36] have shown that  $\text{MnO}_2$  retards the availability of free corrosion products for  
 122 contaminant co-precipitation.

123 The used methodology for the investigation of the process of MB discoloration mechanism by  
 124  $\text{Fe}^0$  consists in following the MB discoloration in the presence of  $\text{MnO}_2$  (“ $\text{Fe}^0$ ” and “ $\text{Fe}^0 + \text{MnO}_2$ ”  
 125 systems). Thus, the availability of corrosion products for MB co-precipitation in the bulk solution  
 126 is delayed by the addition of  $\text{MnO}_2$ . It should be kept in mind that MB discoloration and not MB  
 127 removal is discussed in this study. For the discussion of MB removal TOC measurements for  
 128 instance should have been necessary to account for MB reduction to LMB which remains in  
 129 solution.

## 130 **Materials and Methods**

### 131 **Solutions**

132 The MB molecule has a minimum diameter of approximately 0.9 nm [25,41]. As positively  
 133 charged ions, MB should readily adsorb onto negatively charged surface. That is at  $\text{pH} > \text{pH}_{\text{pzc}}$ ;  
 134  $\text{pH}_{\text{pzc}}$  being the pH at the point of zero charge [42,43]. The used initial concentration was 20 mg

135 L<sup>-1</sup> (~0.063 mM) MB and it was prepared by diluting a 1000 mg L<sup>-1</sup> stock solution. All chemicals  
136 were analytical grade.

### 137 **Solid Materials**

138 The main Fe<sup>0</sup> material (ZVI0 – Tab. 1) is a readily available scrapped iron. Its elemental  
139 composition was found to be: C: 3.52%; Si: 2.12%; Mn: 0.93%; Cr: 0.66%. The material was  
140 fractionated by sieving. The fraction 1.6 – 2.5 mm was used. The sieved Fe<sup>0</sup> was used without  
141 any further pre-treatment. Further 13 commercial Fe<sup>0</sup> samples (ZVI1 through ZVI13) were used  
142 in the set of experiments aiming at characterizing the impact of Fe<sup>0</sup> source. The main  
143 characteristics of these materials are summarized in table 1, which is quite typical for a large  
144 range of powdered and granular Fe<sup>0</sup> used in laboratory investigations and field works.

145 The used granular activated carbon (GAC or AC from LS Labor Service GmbH - Griesheim) was  
146 crushed and sieved. The particle sized fraction ranging from 0.63 to 1.0 mm was used without  
147 further characterization. Granular activated carbon is used as porous adsorbent for MB [25,26].

148 Powdered commercial Fe<sub>2</sub>O<sub>3</sub> (Fluka), Fe<sub>3</sub>O<sub>4</sub> (Fisher Scientific) and MnO<sub>2</sub> (Sigma -Aldrich) were  
149 purchased and used without any further characterization. Fe<sub>2</sub>O<sub>3</sub> and Fe<sub>3</sub>O<sub>4</sub> were also used as  
150 possible MB adsorbents and are proxies for aged iron corrosion products (Tab. 2).

151 Broken manganese nodules (MnO<sub>2</sub>) collected from the deep sea with an average particle size of  
152 1.5 mm and elemental composition of Mn: 41.8%; Fe: 2.40%; Si: 2.41%; Ni: 0.74%; Zn: 0.22%;  
153 Ca: 1.39%; Cu: 0.36% were used. These manganese nodules originated from the Pacific Ocean  
154 (Guatemala- basin: 06°30 N, 92°54 W and 3670 m deep). The target chemically active

155 component is MnO<sub>2</sub>, which occurs naturally mainly as birnessite and todorokite [44]. MnO<sub>2</sub> was  
156 mainly used to control the availability of in situ generated oxides from Fe<sup>0</sup> corrosion [36, 45].

157 Reductive dissolution of MnO<sub>2</sub> has been reported to degrade a number of organic pollutants [39,

158 46 and ref. therein]. Zhu et al. [39] reported the quantitative discoloration of MB by deep sea  
159 manganese nodules (pelagite).

#### 160 **Rationale for Choice of Test Conditions**

161 Materials selected for study were known to be effective for adsorbing MB (GAC), discoloring  
162 MB ( $\text{Fe}^0$ ,  $\text{MnO}_2$ ) or delaying the availability of iron corrosion products in  $\text{Fe}^0/\text{H}_2\text{O}$  systems  
163 ( $\text{MnO}_2$ ).  $\text{Fe}_2\text{O}_3$  and  $\text{Fe}_3\text{O}_4$  were used to characterize the reactivity of aged corrosion products.  
164 Table 2 summarises the function of the individual materials and gives the material surface  
165 coverage in individual reaction vessels. The detailed method for the calculation of the surface  
166 coverage ( $\theta$ ) is presented by Jia et al. [47]. The minima of reported specific surface area (SSA)  
167 values of the adsorbents were used for the estimation of surface coverage. The  $\text{Fe}^0$  SSA was  
168 earlier measured by Mbudi et al. [52]. The value  $120 \text{ \AA}^2$  is considered for the molecular cross-  
169 sectional area of MB [25]. From Tab. 2 it can be seen that, apart from  $\text{Fe}^0$  ( $\theta = 31$ ), all other  
170 materials were present in excess “stoichiometry” ( $\theta \leq 0.2$ ). This means that the available surface  
171 of  $\text{Fe}^0$  can be covered by up to 31 monolayers of MB, whereas the other materials should be  
172 covered only to one fifth with MB ( $\theta = 1$  corresponds to a monolayer coverage). Therefore,  
173 depending on the initial pH value and the affinity of MB for the individual materials ( $\text{pH}_{\text{pzc}}$ ) and  
174 the kinetics of MB diffusion to the reactive sites (material porosity, mixing intensity), the MB  
175 discoloration should be quantitative. A survey of the  $\text{pH}_{\text{pzc}}$  values given in Tab. 2 suggests that  
176 MB adsorption onto all used adsorbents should be favourable because the initial pH was 7.8. At  
177 this pH value all surfaces are negatively charged; MB is positively charged. Because the available  
178  $\text{Fe}^0$  surface can be covered by up to 31 layers of MB, a progressive MB discoloration in presence  
179 of  $\text{Fe}^0$  is expected. The tests were performed under mechanically non-disturbed conditions; the  
180 effect of the shaking intensity was evaluated in separated experiments. Because diffusion is the



181 main mechanism of MB transport under non -disturbed conditions, long reaction times were  
182 experienced to identify the main process of aqueous MB discoloration by  $\text{Fe}^0$ .

### 183 **Discoloration studies**

184 Unless otherwise indicated, batch experiments without shaking were conducted. The batches  
185 consisted of  $5 \text{ g L}^{-1}$  of a reactive material (GAC,  $\text{Fe}^0$ ,  $\text{Fe}_2\text{O}_3$ ,  $\text{Fe}_3\text{O}_4$ ,  $\text{MnO}_2$ ). In some experiments  
186  $5 \text{ g L}^{-1} \text{Fe}^0$  was mixed with 0 or  $5 \text{ g L}^{-1}$  AC and  $\text{MnO}_2$  respectively. An equilibration time of  
187 about 30 days was selected to allow a MB discoloration efficiency of about 80% in the reference  
188 system (ZVI0 alone). The extent of MB discoloration by AC,  $\text{Fe}^0$ ,  $\text{MnO}_2$ , aged ( $\text{Fe}_2\text{O}_3$ ,  $\text{Fe}_3\text{O}_4$ )  
189 and in situ generated iron oxides was characterized. For this purpose 0.11 g of  $\text{Fe}^0$  and 0 or 0.11 g  
190 of the additive were allowed to react in sealed sample tubes containing 22.0 mL of a MB solution  
191 ( $20 \text{ mg L}^{-1}$ ) at laboratory temperature (about  $20^\circ \text{C}$ ). The tubes (20 mL graded) were filled to the  
192 total volume to reduce the head space in the reaction vessels. Initial pH was  $\sim 7.8$ . After  
193 equilibration, up to 5 mL of the supernatant solutions were carefully retrieved (no filtration) for  
194 MB measurements. In order to fit the calibration curve for quantitative measurements, the  
195 maximal dilution factor was four (4).

196 Apart from experiments aiming at investigating the impact of mixing intensity and that of the  
197 initial pH value, the contact vessels were turned over-head at the beginning of the experiment and  
198 allowed to equilibrate in darkness to avoid possible photochemical side reactions. At the end of  
199 the equilibration time no attempt was made to homogenize the solutions.

### 200 **Analytical methods**

201 MB concentrations were determined by a Cary 50 UV -Vis spectrophotometer at a wavelength of  
202 664.5 nm using cuvettes with 1 cm light path. The pH value was measured by combined glass  
203 electrodes (WTW Co., Germany). Electrodes were calibrated with five standards following a  
204 multi-point calibration protocol [53] in agreement with the current IUPAC recommendation [54].

205 Each experiment was performed in triplicate and averaged results are presented.

## 206 **Results and Discussion**

207 After the determination of the residual MB concentration (C) the corresponding percent MB  
208 discoloration was calculated according to the following equation (Eq. 9):

$$209 \quad P = [1 - (C/C_0)] * 100\% \quad (9)$$

210 where  $C_0$  is the initial aqueous MB concentration (about 20 mg L<sup>-1</sup>), while C gives the MB  
211 concentration after the experiment. The operational initial concentration ( $C_0$ ) for each case was  
212 acquired from a triplicate control experiment without additive material (so-called blank). This  
213 procedure was to account for experimental errors during dilution of the stock solution (1000 mg  
214 L<sup>-1</sup>), MB adsorption onto the walls of the reaction vessels and all other possible side reaction  
215 during the experiments.

### 216 **MB discoloration by different agents and discoloration mechanism by Fe<sup>0</sup>**

217 Figure 1 shows the time dependent MB discoloration curve for all the investigated materials. The  
218 reference system is a blank experiment as presented above. It can be seen that commercial Fe<sub>2</sub>O<sub>3</sub>  
219 and MnO<sub>2</sub> did not significantly decolourise MB over the whole duration of the experiments. It is  
220 well-known, that poorly crystalline natural MnO<sub>2</sub> are more reactive than land-born and synthetic  
221 MnO<sub>2</sub> [39,44]. The decreasing order of discoloration efficiency at the end of the experiment was:  
222 Fe<sup>0</sup> > GAC > Fe<sub>3</sub>O<sub>4</sub> > MnO<sub>2</sub>. However, the evolution of the individual systems was very  
223 different.

224 (i) As expected from the surface coverage ( $\theta = 31$ ), Fe<sup>0</sup> presents a progressive MB discoloration  
225 over the duration of the experiment. The discoloration mechanism can be the reduction to LMB  
226 by Fe<sup>0</sup> and Fe<sup>II</sup><sub>(s)</sub> species, adsorption onto in situ generated corrosion products and/or MB co-  
227 precipitation with these new corrosion products.

228 (ii)  $\text{Fe}_3\text{O}_4$  ( $20 \text{ g L}^{-1}$ ) shows a rapid discoloration kinetic for the first 8 days. The discoloration  
229 efficiency then remains constant to approximately 60% through the end of the experiment. This  
230 behaviour is typical for non-porous adsorbents. Alternatively available pores may be inaccessible  
231 for MB.

232 (iii) MB discoloration through GAC is insignificant at the start of the experiment (10% after 10  
233 days) and then increases progressively to 75% at the end of the experiment (day 36). This  
234 behaviour is typical for porous adsorbents.

235 (iv)  $\text{MnO}_{2(\text{nat})}$  shows the same behaviour as GAC but the extent of MB discoloration is  
236 significantly lower (50% at day 36). Natural  $\text{MnO}_2$  acts mostly as adsorbent. MB oxidative  
237 discoloration as reported Zhu et al. [39] is not likely to occur under the experimental conditions  
238 of this work. Note that, on the contrary to Zhu et al. [39], the experiments in this study were  
239 performed under mechanically non-disturbed conditions. While investigating the effect of  
240 dynamic conditions, Zhu et al. [39] did not include any non-disturbed system. They just  
241 compared shaking ( $145 \text{ min}^{-1}$ ) *versus* motor-stirring ( $550 \text{ min}^{-1}$ ) and air-bubbling *versus* nitrogen  
242 bubbling (both  $32 \text{ mL s}^{-1}$ ). These mixing conditions are pertinent to wastewater treatment  
243 systems but are not reproducible in field- $\text{Fe}^0$  treatment walls, mixing could have favour MB  
244 mineralisation (oxidation to  $\text{CO}_2$ ) which is an irreversible discoloration.

245 To better characterize the MB discoloration from aqueous solution by  $\text{Fe}^0$ , five further  
246 experiments have been performed for 36 days with  $5 \text{ g L}^{-1} \text{Fe}^0$  and 0 or  $5 \text{ g L}^{-1}$  of GAC and  
247 natural  $\text{MnO}_2$ .

248 Figure 2a summarizes the results of MB discoloration in these five systems and Fig. 2b depicts  
249 the evolution of MB discoloration for  $5 \text{ g L}^{-1} \text{Fe}^0$  and additive (AC or  $\text{MnO}_2$ ) dosages varying  
250 from 0 to  $9 \text{ g L}^{-1}$  for an experimental duration of 36 days. Fig. 2a shows a regular evolution for  
251 the systems involving AC and  $\text{Fe}^0$ . The MB discoloration efficiency decreases in the order “ $\text{Fe}^0 +$

252 AC” > Fe<sup>0</sup> > AC. Considering AC and Fe<sup>0</sup> as pure adsorbents it is expected that the mixture  
 253 (maximal available binding sites) depicts a larger MB discoloration efficiency than individual  
 254 materials (Tab. 2). This trend was not observed for systems involving MnO<sub>2</sub>. Here, the  
 255 decreasing order of MB discoloration efficiency was: Fe<sup>0</sup> > “Fe<sup>0</sup> + MnO<sub>2</sub>” ≅ MnO<sub>2</sub>. These  
 256 observations were described by Noubactep et al. [36,45,55] for uranium removal by Fe<sup>0</sup>. A  
 257 “MnO<sub>2</sub> test” was proposed for mechanistic investigations in Fe<sup>0</sup>/H<sub>2</sub>O systems. The major feature  
 258 of the “MnO<sub>2</sub> test” is that in reacting with Fe<sup>II</sup> from Fe<sup>0</sup> oxidation, MnO<sub>2</sub> delays the availability  
 259 of “free” corrosion products which entrapped contaminants while polymerising and precipitating.  
 260 “Free” corrosion products are Fe-oxides generated in the vicinity of metallic iron grains. As long  
 261 as MnO<sub>2</sub> is reductively dissolved, Fe-oxides are generated at its surface or in its vicinity.  
 262 Thereafter, if co-precipitation is the primary mechanism of contaminant removal, no quantitative  
 263 removal could occur until enough free corrosion products are available to entrap them while  
 264 ageing [36]. To confirm this statement the experiment presented in Fig. 2b was conducted.  
 265 From Fig. 2b it can be seen that about 4 g L<sup>-1</sup> activated carbon are sufficient to achieve almost  
 266 100% MB discoloration. For [AC] > 4 g L<sup>-1</sup> no additional discoloration was possible. The system  
 267 with MnO<sub>2</sub> depicts a progressive decrease of MB discoloration with increasing MnO<sub>2</sub> mass  
 268 loading. The reaction of Fe<sup>II</sup> species yielding reductive dissolution of MnO<sub>2</sub> is well documented  
 269 [37,40,56] and yields more adsorbents (e.g., FeOOH, MnOOH – Eq. 7 and 8). However, MB  
 270 discoloration is only quantitative when the oxidative capacity of available MnO<sub>2</sub> for Fe<sup>II</sup> is  
 271 exhausted. Thus, MB is removed from the aqueous solution through co-precipitation with in situ  
 272 generated iron corrosion products. The characterization of the impact of MnO<sub>2</sub> on contaminant  
 273 removal by Fe<sup>0</sup> occurs ideally under non-disturbed conditions [57]. Note that, if the experiments  
 274 are performed under (too high) mixing conditions or in columns, increased contaminant removal  
 275 efficiency in the presence of MnO<sub>2</sub> could have been reported. For example, Burghardt and

276 Kassahun [58] reported increased uranium and radium removal in “Fe<sup>0</sup> + MnO<sub>2</sub>” systems  
277 comparatively to the system with Fe<sup>0</sup> alone. The results of Burghardt and Kassahun [58] are by  
278 no means contradictory to those reported here and elsewhere [40] because the net effect of MnO<sub>2</sub>  
279 is to promote iron hydroxide formation (or to sustain corrosion) resulting in an increased  
280 contaminant removal capacity. Similarly, while Noubactep et al. [36,45,57] reported a delay of U  
281 removal by Fe<sup>0</sup> in the presence of pyrite in non-disturbed experiments, Lipczynska-Kochany et  
282 al. [59] reported increased carbon tetrachloride degradation in the presence of pyrite. Pyrite is  
283 known for its pH lowering capacity, and thus increasing iron corrosion. Non-disturbed  
284 experiments allow a better characterization of the progression of involved processes.

#### 285 **Effect of Fe<sup>0</sup> source**

286 Experiments were conducted with 14 different Fe<sup>0</sup> materials: ZVI0 through ZVI13. ZVI1, ZVI2,  
287 ZVI3 and ZVI12 were powdered materials. The 10 other samples were granulated materials. The  
288 results of MB discoloration are summarised in table 1. The experimental duration was 35 days. It  
289 is shown that powdered materials are more efficient in removing MB than granulated materials  
290 (Tab. 1). The discoloration efficiency for granulated materials varies from 65% for ZVI7 to 80%  
291 for ZVI2 (absolute values). That is 15% reactivity difference while the maximum standard  
292 deviation for the triplicates in individual experiments was 8.5% (for ZVI12). Therefore, the Fe<sup>0</sup>  
293 source (intrinsic reactivity) is a significant operational parameter for laboratory studies. Similar  
294 results were reported by Miehr et al. [60] who reported differences in rate constants of contaminant  
295 reduction up to four orders of magnitude when comparing nine types of Fe<sup>0</sup>. Therefore,  
296 comparing results obtained with different granulated Fe<sup>0</sup> under comparable experimental  
297 conditions may lead to erroneous conclusions.

## 298 **Effect of shaking intensity**

299 Figure 3 clearly shows that MB discoloration efficiency increases with the shaking intensity. The  
300 experimental duration was 24 h (1 day). The reaction vessels were shaken on a rotary shaker. The  
301 MB discoloration rate of 5% at 0 min<sup>-1</sup> (non-disturbed conditions) increased to 96% at 200 min<sup>-1</sup>.  
302 Between 100 and 150 min<sup>-1</sup> the MB discoloration rate was constant to 55%. Parallel experiments  
303 in 100 mL Erlenmeyer shows comparative results but at 200 min<sup>-1</sup> the solution was no more  
304 limp and depicted a brown coloration that persisted even after the solutions were allowed to  
305 settle for 5 hours. Therefore, a mixing intensity of about 150 min<sup>-1</sup> can be seen as the critical  
306 intensity below which MB discoloration studies should be performed. Since applied mixing  
307 intensities have not been tested in preliminary works, it is likely that some used mixing  
308 operations have been too massive and impractical to mimic subsurface conditions [11]. Mixing  
309 intensities as higher as 500 min<sup>-1</sup> [61,62] have been used to “keep the iron powder suspended”.  
310 Generally, Fe<sup>0</sup>-based materials show greater contaminant removal efficiency under mixed than  
311 under non-disturbed conditions. This removal efficiency is usually attributed to direct reduction  
312 whenever the thermodynamics are favourable. However, the open literature on mixed batch  
313 experiments demonstrates that a minimum mixing intensity (bubbling, shaking or stirring) is  
314 required for complete suspension of solid particles in a liquid medium (e.g., an aqueous solution).  
315 Below this critical mixing intensity, the total surface area of the investigated particles is not  
316 directly accessible for reaction and the rate of mass transfer depends strongly on stirring rate.  
317 Kinetic studies aiming at distinguishing between diffusion-controlled and chemistry-controlled  
318 processes have to be conducted at mixing intensities above this critical value [56]. Noubactep  
319 [11] has demonstrated that experiments in Fe<sup>0</sup>/H<sub>2</sub>O systems aiming at investigating processes  
320 pertinent to subsurface situations should be conducted below the critical value (mass transfer  
321 dependent). For Fe<sup>0</sup>, it is obvious, that the value of this critical mixing intensity depends on the

322 particle size (nm,  $\mu\text{m}$ , mm). Choe et al. [63] reported a critical value of  $40 \text{ min}^{-1}$  for nano-scale  
323  $\text{Fe}^0$  and performed their experiments at a mixing intensity of  $60 \text{ min}^{-1}$ . According to the  
324 presentation above, Choe et al. [63] would have worked with mixing intensities below  $40 \text{ min}^{-1}$  to  
325 obtain results relevant for groundwater conditions. Furthermore, working at mixing intensities  
326 above  $40 \text{ min}^{-1}$  accelerates iron corrosion yielding more corrosion products which are equally  
327 kept suspended in the reaction medium. In the course of corrosion products formation,  
328 contaminants are entrapped in the matrix of iron oxides (co-precipitation). It is well known that  
329 even low adsorbable species are readily removed from aqueous solutions when precipitation  
330 occurs in their presence [16,17,20,21]. As discussed above, MB discoloration mainly occurs  
331 through co-precipitation with newly generated corrosion products (see above: “MB discoloration  
332 by different agents and discoloration mechanism by  $\text{Fe}^0$ ”). MB discoloration by aged corrosion  
333 products was insignificant ( $\text{Fe}_2\text{O}_3$ ) or very limited ( $\text{Fe}_3\text{O}_4$ ).

#### 334 **Effect of the initial pH value**

335 The effect of the initial pH on MB discoloration was investigated over the pH range of 1.5 to  
336 10.0. The initial pH was adjusted by addition of 1.0 M NaOH or HCl. The experiments were  
337 conducted under shaken conditions ( $100 \text{ min}^{-1}$ ). The pH of the solutions was monitored at the end  
338 of the experiments (24 and 48 h). The results are summarised in Fig. 4. MB discoloration was  
339 negligible when the final pH was lower than 4 ( $P < 10\%$ ). Once the final pH exceeded this  
340 critical value, MB quantitative discoloration occurred and the extent was pH-independent (60%  
341 after 24 h and 76% after 48 h). This observation is consistent with the two main types of aqueous  
342 iron corrosion under oxic conditions [64,65] : (i) hydrogen evolution type ( $\text{pH} < 4$ ) and (ii) oxygen  
343 absorption type ( $\text{pH} > 4$ ). The characteristic feature of “hydrogen evolution corrosion” is the  
344 liberation of hydrogen as hydrogen gas ( $\text{H}_2$ ) at the cathode. Hydrogen evolution corrosion is  
345 normally associated with acid electrolytes (e.g., acid mine drainage) and is not relevant for the

346 majority of groundwaters, unless the aquifer is strictly anoxic. The “oxygen absorption” type of  
347 immersed Fe<sup>0</sup> corrosion is characteristic of neutral waters. At these pH values (pH > 4.0) iron  
348 solubility is low [66]. Thus iron oxide precipitates and MB are removed from the aqueous  
349 solution by sequestration (co-precipitation). The results from Fig. 4 validate the concept that all  
350 contaminants are primarily adsorbed or/and sequestered by iron corrosion products (co-  
351 precipitation) [11,12]. In fact MB discoloration was quantitative only at final pH > 4, where iron  
352 oxides precipitate due to the low solubility of Fe. Within the oxide film, redox reactions driven  
353 by Fe<sup>II</sup> species have been reported [67]. Therefore, co-precipitated MB can be reduced to LMB  
354 but this reaction could not contribute to recorded MB discoloration.

355 A certain commonly misconception may be found in the literature concerning the process of  
356 contaminant removal in Fe<sup>0</sup>/H<sub>2</sub>O systems due to improper consideration of the two main  
357 mechanisms of iron corrosion. Ideally, whenever the initial pH is lower than 4, the pH should be  
358 carefully monitored and used to interpret results. From Fig. 4 it can be seen for example, that for  
359 an initial pH of 3.0 the final pH was 4.3 and the extent of MB discoloration was slightly lower  
360 than that of the experiment with initial pH values ≥ 4 (for the given experimental duration).

361 Consequently, the repeatedly reported lag time for contaminant removal [61,68] is the time to  
362 exceed pH 4 (or to enable generation of enough corrosion products for contaminant co-  
363 precipitation/sequestration). It must be emphasised that for contaminants (e.g., Cr<sup>IV</sup>) which are  
364 also reducible by aqueous Fe<sup>II</sup> the extent of their removal at pH < 4 depends on their relative  
365 solubility of their reduced form. Regardless of their redox reactivity co-precipitation of  
366 contaminant and reaction products occurs at pH > 4. Contaminants, intermediates and final  
367 products are possibly entrapped in the matrix of corrosion products.



### 368 **Effect of solution chemistry**

369 The effect of solution parameters on MB discoloration by  $\text{Fe}^0$  was studied using 0.2 mM of  
370  $\text{Al}(\text{NO})_3$ ,  $\text{BaCl}_2$ ,  $\text{CaCl}_2$ ,  $\text{CuCl}_2$ , EDTA,  $(\text{NH}_4)_2\text{CO}_3$ , and  $\text{NiCl}_2$ . Further non-disturbed  
371 experiments were performed for 35 days with concentrations of  $\text{CaCl}_2$ ,  $\text{CuCl}_2$  and  $\text{NaHCO}_3$   
372 varying from 0 to 4 mM (Figure 5). Figure 5a shows that apart from  $(\text{NH}_4)_2\text{CO}_3$  (90%) all other  
373 additives lower the extent of MB discoloration by  $\text{Fe}^0$  (78%). The lowest discoloration efficiency  
374 (15%) was observed in the presence of EDTA and is consistent with the fact that complexing  
375  $\text{Fe}^{\text{II}}/\text{Fe}^{\text{III}}$  delays the iron oxide precipitation [69 -71] and hence retards MB discoloration. For the  
376 four systems containing chloride ions ( $\text{Cl}^-$ ),  $\text{NiCl}_2$  depicts the lowest MB discoloration efficiency  
377 (33%) and  $\text{CaCl}_2$  the highest (72%).  $\text{BaCl}_2$  and  $\text{CuCl}_2$  show very comparable discoloration  
378 efficiency (about 60%). This observation is partly consistent with reported results from the  
379 literature on corrosion stating that: (i) at low concentration  $\text{CO}_2^{3-}$  is corrosive, (ii) hardness ( $\text{Ca}^{2+}$ )  
380 is corrosive, while  $\text{Ni}^{2+}$  has inhibitive properties for iron corrosion.  $\text{Cu}^{2+}$  would have accelerated  
381  $\text{Fe}^0$  corrosion yielding more corrosion products for MB discoloration than in the reference system  
382 ( $\text{Fe}^0$  alone). Because this was not the case, the experiments reported in Fig. 5b were performed.  
383 It can be seen that  $\text{NaHCO}_3$  enhances MB discoloration for all tested concentrations. The  
384 discoloration efficiency increased from 77% at 0.0 mM  $\text{NaHCO}_3$  to 90% at 0.8 mM  $\text{NaHCO}_3$  and  
385 remains constant for higher  $\text{NaHCO}_3$  concentrations ( $\leq 4$  mM). In the experiments with  $\text{CaCl}_2$   
386 and  $\text{CuCl}_2$  the initial discoloration rate of 77% first decreases to 70 and 64% respectively at an  
387 additive concentration of 0.2 mM and subsequently increases to about 74% and remains constant.  
388 However, for 4 mM  $\text{CuCl}_2$  the discoloration efficiency (73% at 2 mM) drops to 30% at 4 mM  
389 while the discoloration efficiency in the presence of  $\text{CaCl}_2$  remains constant (74%). The  
390 behaviour of the system with  $\text{CuCl}_2$  was not further investigated but suggests that if  $\text{Cu}^{2+}$  is  
391 quantitatively produced in a Cu/Fe bimetallic system the reactivity of  $\text{Fe}^0$  may be inhibited. This

392 issue is yet to be considered in the  $\text{Fe}^0$  technology. Similarly, the comparatively low discoloration  
393 efficiency observed in the system with 0.2 mM  $\text{NiCl}_2$  (33% against 60% for  $\text{CaCl}_2$ ) should  
394 question the concept of using Ni and Cu as additive metals to form nickel bimetallic systems to  
395 “improve the reduction capacity of  $\text{Fe}^0$ ” [28]. No such improvement could be observed in this  
396 study (Fig. 5). Discussing the validity of the concept of using bimetals to improve  $\text{Fe}^0$   
397 reactivity is over the scope of this work (see ref. [72]).

398 Another important issue from the discussion above is the importance of the cation nature in  
399 chloride salts on the extent of MB removal. Generally, chloride ions are known to promote iron  
400 corrosion, and therefore increase, sustain or restore  $\text{Fe}^0$  reactivity. These observations are mostly  
401 attributed to pitting iron corrosion or avoiding the formation of oxide-layers on iron [73, 74]. The  
402 discussion above demonstrated clearly that the nature of the used salt should be considered in  
403 comparing results from independent sources.

#### 404 **Conclusions**

405 In summary, despite the low adsorptivity exhibited by MB towards  $\text{Fe}^0$ ,  $\text{Fe}_2\text{O}_3$  and  $\text{Fe}_3\text{O}_4$ , under  
406 the experimental conditions, MB was quantitatively discolored as  $\text{Fe}^0$  corrosion proceeded. The  
407 extent of MB discoloration was insignificant in experiments in which the availability of in situ  
408 generated corrosion products was delayed ( $\text{MnO}_2$  addition). Data from the experiments with the  
409 systems “ $\text{Fe}^0$ ” and “ $\text{MnO}_2$ ” clearly showed that the kinetics of MB adsorption and reduction by  
410  $\text{MnO}_2$  is slower than MB co-precipitation. Thus, even in systems where direct contaminant  
411 reduction (electrons from  $\text{Fe}^0$ ) is likely to occur, co-precipitation will interfere with (or even  
412 hamper) mass transport involving  $\text{Fe}^0$ .

413 The concept that methylene blue (MB) discoloration from aqueous solution in presence of  
414 metallic iron is caused by MB co-precipitation with  $\text{Fe}^0$  corrosion products is consistent with  
415 many experimental observations, in particular the effects of the initial pH value and the impact of

416  $\text{MnO}_2$  on MB discoloration. Generally, a aqueous contaminant removal in  $\text{Fe}^0/\text{H}_2\text{O}$  systems can be  
417 viewed as a “trickle down” in which a fraction of the targeted contaminant is continuously adsorb  
418 onto in situ generated high reactive corrosion products [11]. Contaminants are subsequently  
419 entrapped into the structure of ageing corrosion products. In this situation, no observable  
420 equilibrium is attained. Therefore, the use of adsorption isotherms (e.g., Freundlich, Langmuir) to  
421 interpret data from removal experiments in  $\text{Fe}^0/\text{H}_2\text{O}$  systems is not justified (e.g. ref. [75]).  
422 Furthermore, adsorbed or co-precipitated contaminants can be further reduced both by a direct  
423 and an indirect mechanism [11,12]. The direct contaminant reduction is only possible when the  
424 oxide-film on  $\text{Fe}^0$  is electronic conductive or if so-called electron mediators are available [34,  
425 76]. Noubactep [11] has clearly shown that the concept of contaminant adsorption and co-  
426 precipitation as fundamental removal mechanism is more accurate and considers inherent  
427 mistakes of the reductive transformation concept.

428 It must be concluded that natural  $\text{Fe}^0/\text{H}_2\text{O}$  systems consist of core  $\text{Fe}^0$  and essentially amorphous  
429 Fe oxides that remain to be characterized. In this regard, many investigators have shown the  
430 presence of various Fe oxyhydroxides and discussed their role in the process of contaminant  
431 removal [77 -82]. Strictly, these oxyhydroxides should be considered as transient states as  
432  $\text{Fe}^0/\text{H}_2\text{O}$  systems are transforming systems. Therefore, a continuously reacting  $\text{Fe}^0/\text{H}_2\text{O}$  system  
433 can not be simply treated being at thermodynamic equilibrium. Thus, characterising the system  
434 composition at certain dates is very useful but should be completed by continuously  
435 characterizing the system as the contaminants are removed and/or transformed.

436 With this study, the potential of bulk reactions with selected additives for providing mechanistic  
437 information [36] on aqueous contaminant removal is confirmed for the first time using an organic  
438 compound. This study also demonstrates the significant impact of selected operational  
439 experimental parameters (iron type, shaking intensity, solution chemistry) on the process of MB

440 co-precipitation in Fe<sup>0</sup>/H<sub>2</sub>O systems. A unified experimental procedure is needed to : (i) avoid  
441 further data generation under non relevant experimental conditions , and (ii) facilitate the inter -  
442 laboratory comparison of data. At the term such efforts will provide a confident background for a  
443 non-site-specific iron barrier design [83] . Keeping in mind the large spectrum of contaminants  
444 that can be removed in Fe<sup>0</sup>/H<sub>2</sub>O systems and the diversity of Fe<sup>0</sup> materials that are used by  
445 individual research groups, it is obvious, that the development of such an unified experimental  
446 procedure should be a concerted effort.

#### 447 **Acknowledgments**

448 For providing the iron materials (Fe<sup>0</sup>) investigated in this study the author would like to express  
449 his gratitude to the branch of the MAZ (Metallaufbereitung Zwickau, Co) in Freiberg (Germany),  
450 Gotthart Maier Metallpulver GmbH (Rheinfelden, Germany), Connelly GPM Inc. (USA), Dr. R.  
451 Köber from the Institute Earth Science of the University of Kiel and Dr. -Ing. V. Biermann from  
452 the Federal Institute for Materials Research and Testing (Berlin, Germany). Mechthild Rittmeier  
453 and Emin Özden are acknowledged for technical support. The work was granted by the Deutsche  
454 Forschungsgemeinschaft (DFG-No 626/2-2).

455

#### 456 **References**

- 457 [1] A.D. Henderson, A.H. Demond, Long -term performance of zero -valent iron permeable  
458 reactive barriers: a critical review. *Environ. Eng. Sci.* 24 (2007), 401–423.
- 459 [2] D.F. Laine, I.F. Cheng, The destruction of organic pollutants under mild reaction conditions:  
460 A review. *Microchem. J.* 85 (2007), 183–193.
- 461 [3] S.F. O'Hannesin, R.W. Gillham, Long-term performance of an in situ "iron wall" for  
462 remediation of VOCs. *Ground Water* 36 (1998), 164–170.

- 463 [4] M.M. Scherer, S. Richter, R.L. Valentine, P.J.J. Alvarez, Chemistry and microbiology of  
464 permeable reactive barriers for in situ groundwater clean up. *Rev. Environ. Sci. Technol.* 30  
465 (2000), 363–411.
- 466 [5] P.G. Tratnyek, M.M. Scherer, T.J. Johnson, L.J. Matheson, Permeable reactive barriers of  
467 iron and other zero-valent metals. In *Chemical Degradation Methods for Wastes and*  
468 *Pollutants: Environmental and Industrial Applications*, Tarr, M.A., Ed., Marcel Dekker: New  
469 York, (2003) 371–421.
- 470 [6] N.A. VanStone, R.M. Focht, S.A. Mabury, B.S. Lollar, Effect of iron type on kinetics and  
471 carbon isotopic enrichment of chlorinated ethylenes during abiotic reduction on Fe(0).  
472 *Ground Water* 42 (2004), 268–276.
- 473 [7] S.D. Warner, D. Sorel, Ten years of permeable reactive barriers: Lessons learned and future  
474 expectations. In: *Chlorinated Solvent and DNAPL Remediation: Innovative Strategies for*  
475 *Subsurface Cleanup*, Henry, S.M., Warner, S.D., Eds, American Chemical Society:  
476 Washington, DC, ACS Symp., Ser. 837 (2003), 36–50.
- 477 [8] Y. You, J. Han, P.C. Chiu, Y. Jin, Removal and inactivation of waterborne viruses using  
478 zerovalent iron. *Environ. Sci. Technol.* 39 (2005), 9263–9269.
- 479 [9] B. Jafarpour, P.T. Imhoff, P.C. Chiu, Quantification and modelling of 2,4-dinitrotoluene  
480 reduction with high-purity and cast iron. *J. Contam. Hydrol.* 76 (2005), 87–107.
- 481 [10] J.A. Mielczarski, G.M. Atenas, E. Mielczarski, Role of iron surface oxidation layers in  
482 decomposition of azo-dye water pollutants in weak acidic solutions. *Appl. Catal. B56* (2005),  
483 289–303.
- 484 [11] C. Noubactep, Processes of contaminant removal in “Fe<sup>0</sup>-H<sub>2</sub>O” systems revisited. The  
485 importance of co-precipitation. *Open Environ. J.* 1 (2007), 9–13.

- 486 [12] C. Noubactep, A critical review on the mechanism of contaminant removal in Fe<sup>0</sup>-H<sub>2</sub>O  
487 systems. *Environ. Technol.* 29 (2008), 909–920.
- 488 [13] M. Cohen, The formation and properties of passive films on iron. *Can. J. Chem.* 37 (1959),  
489 286–291.
- 490 [14] K.J. Vetter, General kinetics of passive layers on metals. *Electrochim. Acta* 16 (1971),  
491 1923–1937.
- 492 [15] B. Gu, J. Schmitt, Z. Chen, L. Liang, J.F. McCarthy, Adsorption and desorption of natural  
493 organic matter on iron oxide: mechanisms, and models. *Environ. Sci. Technol.* 28 (1994), 38–  
494 46.
- 495 [16] Y. Satoh, K. Kikuchi, S. Kinoshita, H. Sasaki, Potential capacity of coprecipitation of  
496 dissolved organic carbon (DOC) with iron(III) precipitates. *Limnology* 7 (2006), 231–235.
- 497 [17] U. Schwertmann, F. Wagner, H. Knicker, Ferrihydrite–Humic associations magnetic  
498 hyperfine interactions. *Soil Sci. Soc. Am. J.* 69 (2005), 1009–1015.
- 499 [18] W.-C. Ying, J.J. Duffy, M.E. Tucker, Removal of humic acid and toxic organic compounds  
500 by iron precipitation. *Environ. Progr.* 7 (1988), 262–269.
- 501 [19] E. Tipping, The adsorption of aquatic humic substances by iron oxides. *Geochim.*  
502 *Cosmochim. Acta* 45 (1981), 191–199.
- 503 [20] E. Tipping, Some aspects of the interactions between particulate oxides and aquatic humic  
504 substances. *Mar. Chem.* 18 (1986), 161–169.
- 505 [21] R.J. Crawford, I.H. Harding, D.E. Mainwaring, Adsorption and coprecipitation of single  
506 heavy metal ions onto the hydrated oxides of iron and chromium. *Langmuir* 9 (1993), 3050–  
507 3056.
- 508 [22] H. Füredi-Milhofer, Spontaneous precipitation from electrolytic solutions. *Pure Appl. Chem.*  
509 53 (1981), 2041–2055.

- 510 [23] I. Nirdosh, S.V. Muthuswami, M.H.I. Baird Radium in uranium mill tailings - Some  
511 observations on retention and removal. *Hydrometallurgy* 12 (1984), 151–176.
- 512 [24] B.D. Jones, J.D. Ingle, Evaluation of redox indicators for determining sulfate-reducing and  
513 dechlorinating conditions. *Water Res.* 39 (2005), 4343–4354.
- 514 [25] A.A. Attia, B.S. Girgis, N.A. Fathy, Removal of methylene blue by carbons derived from  
515 peach stones by H<sub>3</sub>PO<sub>4</sub> activation: Batch and column studies. *Dyes and Pigments* 76 (2008),  
516 282–289.
- 517 [26] J. Avom, J.B. Ketcha, C. Noubactep, P. Germain, Adsorption of methylene blue from an  
518 aqueous solution onto activated carbons from palm-tree cobs. *Carbon* 35 (1997), 365–369.
- 519 [27] Dutta, K., Mukhopadhyay, S., Bhattacharjee, S., Chaudhuri, B., 2001. Chemical oxidation of  
520 methylene blue using a Fenton-like reaction. *J. Hazard. Mater.* 84, 57–71.
- 521 [28] L.M. Ma, Z.G. Ding, T.Y. Gao, R.F. Zhou, W.Y. Xu, J. Liu, Discoloration of methylene  
522 blue and wastewater from a plant by a Fe/Cu bimetallic system. *Chemosphere* 55 (2004),  
523 1207–1212.
- 524 [29] S. Pande, S.K. Ghosh, S. Nath, S. Praharaj, S. Jana, S. Panigrahi, S. Basu, T., Pal, Reduction  
525 of methylene blue by thiocyanate: Kinetic and thermodynamic aspects. *J. Colloid Interf.*  
526 *Sci.* 299 (2006), 421–427.
- 527 [30] K. Imamura, E. Ikeda, T. Nagayasu, T. Sakiyama, K. Nakanishi, Adsorption behavior of  
528 methylene blue and its congeners on a stainless steel surface. *J. Colloid Interf. Sci.* 245  
529 (2002), 50–57.
- 530 [31] E.E. Oguzie, Corrosion inhibition of mild steel in hydrochloric acid solution by methylene  
531 blue dye. *Mater. Lett.* 59 (2005), 1076–1079.
- 532 [32] J. Cao, L. Wei, Q. Huang, L. Wang, S. Han, Reducing degradation of azo dye by zero-valent  
533 iron in aqueous solution. *Chemosphere* 38 (1999), 565–571.

- 534 [33] S. Nam, P.G. Tratnyek, Reduction of azo dyes with zero-valent iron. *Wat. Res.* 34 (2000),  
535 1837–1845.
- 536 [34] E.J. Weber, Iron-mediated reductive transformations: Investigation of reaction mechanism.  
537 *Environ. Sci. Technol.* 30 (1996), 716–719.
- 538 [35] F. dos Santos Coelho, J.D. Ardisson, F.C.C. Moura, R.M. Lago, E. Murad, J.D. Fabris,  
539 Potential application of highly reactive Fe(0)/Fe<sub>3</sub>O<sub>4</sub> composites for the reduction of Cr(VI)  
540 environmental contaminants. *Chemosphere* 71 (2008), 90–96.
- 541 [36] C. Noubactep, G. Meinrath, J.B. Merkel, Investigating the mechanism of uranium removal  
542 by zerovalent iron materials. *Environ. Chem.* 2 (2005), 235–242.
- 543 [37] D. Postma, C.A.J. Appelo, Reduction of Mn-oxides by ferrous iron in a flow system: column  
544 experiment and reactive transport modelling. *Geochim. Cosmochim. Acta* 64 (2000), 1237 –  
545 1247.
- 546 [38] A.F. White, M.L. Paterson, Reduction of aqueous transition metal species on the surface of  
547 Fe(II)-containing oxides. *Geochim. Cosmochim. Acta* 60 (1996), 3799–3814.
- 548 [39] M.-X. Zhu, Z. Wang, L. -Y. Zhou, Oxidative decolorization of methylene blue using  
549 pelagite. *J. Hazard. Mater.* 150 (2008), 37–45.
- 550 [40] D.F.A. Koch, Kinetics of the reaction between manganese dioxide and ferrous ion. *Aust. J.*  
551 *Chem* 10 (1957), 150–159.
- 552 [41] H. Valdes, M. Sanchez-Polo, J. Rivera-Utrilla, C.a. Zaror, Effect of ozone treatment on  
553 surface properties of activated carbon. *Langmuir* 18 (2002), 2111–2116.
- 554 [42] V. Ender, Zur Struktur der Phasengrenze Metalloxid/Elektrolyt -Potentialbildung und  
555 Ladungsbilanz. *Acta Hydrochim. Hydrobiol.* 19 (1991), 199–208.
- 556 [43] M.R. Hoffmann, S.T. Martin, W. Choi, D.W. Bahnemann, Environmental applications of  
557 semiconductor photocatalysis. *Chem. Rev.* 95 (1995), 69–96.



- 558 [44] J.E. Post, Manganese oxide minerals: Crystal structures and economic and environmental  
559 significance. *Proc. Natl. Acad. Sci. USA* 96 (1999), 3447–3454.
- 560 [45] C. Noubactep, A. Schöner, G. Meinrath, Mechanism of uranium (VI) fixation by elemental  
561 iron. *J. Hazard. Mater.* 132 (2006), 202–212.
- 562 [46] H. Zhang, C. -H. Huang, Oxidative transformation of triclosan and chl orophene by  
563 manganese oxides. *Environ. Sci. Technol.* 37 (2003), 2421–2430.
- 564 [47] Y. Jia, P. Aagaard, G.D. Breedveld, Sorption of triazoles to soil and iron minerals.  
565 *Chemosphere* 67 (2007), 250–258.
- 566 [48] T. Liu, D.C.W. Tsang, I.M.C. Lo, Chromium(VI) reduction kinetics by zero -valent iron in  
567 moderately hard water with humic acid: iron dissolution and humic acid adsorption. *Environ.*  
568 *Sci. Technol.* 42 (2008), 2092–2098.
- 569 [49] K. Hanna, Adsorption of aromatic carboxylate compounds on the surface of synthesized iron  
570 oxide-coated sands. *Appl. Geochem.* 22 (2007), 2045–2053.
- 571 [50] S. Yean, L. Cong., C.T. Yavuz, J.T. Mayo, W.W. Yu, A.T. Kan, V.L. Colvin, M.B. Tomson,  
572 Effect of magnetite particle size on adsorption and desorption of arsenite and arsenate. *J.*  
573 *Mater. Res.* 20 (2005), 3255–3264.
- 574 [51] M.I. Bautista -Toledo, J.D. Méndez -Díaz, M. Sánchez -Polo, J. Rivera -Utrilla, M.A. Ferro -  
575 García, Adsorption of sodium dodecylbenzenesulfonate on activated carbons: Effects of  
576 solution chemistry and presence of bacteria. *J. Colloid Interf. Sci.* 317 (2008), 11–17.
- 577 [52] C. Mbudi, P. Behra, B. Merkel, The Effect of Background Electrolyte Chemistry on  
578 Uranium Fixation on Scrap Metallic Iron in the Presence of Arsenic. Paper presented at the  
579 Inter. Conf. Water Pollut. Natural Porous Media ( WAPO2), Barcelona (Spain) April 11 – 13  
580 (2007), 8 pages.

- 581 [53] G. Meinrath, P. Spitzer, Uncertainties in determination of pH. *Mikrochem. Acta* 135 (2000),  
582 155–168.
- 583 [54] R.P. Buck, S. Rondinini, A.K. Covington, F.G.K. Baucke, C.M.A. Brett, M.F. Camoes,  
584 M.J.T. Milton, T. Mussini, R. Naumann, K.W. Pratt, P. Spitzer, G.S. Wilson, Measurement of  
585 pH. Definition, standards, and procedures (IUPAC Recommendations 2002), *Pure Appl.*  
586 *Chem.* 74 (2002), 2169–2200.
- 587 [55] C. Noubactep, G. Meinrath, P. Dietrich, B. Merkel, Mitigating uranium in ground water:  
588 prospects and limitations. *Environ. Sci. Technol.* 37 (2003), 4304–4308.
- 589 [56] T. Tekin, M. Bayramoglu, Kinetics of the reduction of  $\text{MnO}_2$  with  $\text{Fe}^{2+}$  ions in acidic  
590 solutions. *Hydrometallurgy* 32 (1993), 9–20.
- 591 [57] C. Noubactep, Investigations for the passive in-situ Immobilization of Uranium (VI) from  
592 Water (in German). Dissertation, TU Bergakademie Freiberg, *Wiss. Mitt. Institut für*  
593 *Geologie der TU Bergakademie Freiberg, Band 21* (2003), 140 pp, ISSN1433-1284.
- 594 [58] D. Burghardt, A. Kassahun, Development of a reactive zone technology for simultaneous in  
595 situ immobilisation of radium and uranium. *Environ. Geol.* 49 (2005), 314–320.
- 596 [59] E. Lipczynska-Kochany, S. Harms, R. Milburn, G. Sprah, N. Nadarajah, Degradation of  
597 carbon tetrachloride in the presence of iron and sulphur containing compounds. *Chemosphere*  
598 29 (1994), 1477–1489.
- 599 [60] R. Miehr P.G. Tratnyek, Z.J. Bandstra, M.M. Scherer, J.M. Alowitz, J.E. Bylaska, Diversity  
600 of contaminant reduction reactions by zerovalent iron: Role of the reductate. *Environ. Sci.*  
601 *Technol.* 38 (2004), 139–147.
- 602 [61] Z. Hao, X. Xu, D. Wang, Reductive denitrification of nitrate by scrap iron filings. *J.*  
603 *Zhejiang Univ. Sci.* 6B (2005), 182–187.

- 604 [62] W.S. Pereira, R.S. Freire, Azo dye degradation by recycled waste zero-valent iron powder. J.  
605 Braz. Chem. Soc. 17 (2006), 832–838.
- 606 [63] S. Choe, Y.Y. Chang, K.Y. Hwang, J. Khim, Kinetics of reductive denitrification by  
607 nanoscale zero-valent iron, Chemosphere 41 (2000), 1307–1311.
- 608 [64] G.W. Whitman, R.P. Russel, V.J. Altieri, Effect of hydrogen ion concentration on the  
609 submerged corrosion of steel. Indust. Eng. Chem. 16 (1924), 665–670.
- 610 [65] E.R. Wilson, The Mechanism of the corrosion of iron and steel in natural waters and the  
611 calculation of specific rates of corrosion. Indust. Eng. Chem. 15 (1923), 127–133.
- 612 [66] D. Rickard, The solubility of FeS. Geochim. Cosmochim. Acta 70 (2006), 5779–5789.
- 613 [67] M. Stratmann, J. Müller, The mechanism of the oxygen reduction on rust covered metal  
614 substrates. Corros. Sci. 36 (1994), 327–359.
- 615 [68] C.G. Schreier, M. Reinhard, Transformation of chlorinated organic compounds by iron and  
616 manganese powders in buffered water and in landfill leachate. Chemosphere 29 (1994),  
617 1743–1753.
- 618 [69] L.J. Matheson, P.G. Tratnyek, Reductive dehalogenation of chlorinated methanes by iron  
619 metal. Environ. Sci. Technol. 28 (1994), 2045–2053.
- 620 [70] C. Noubactep, G. Meinrath, P. Dietrich, M. Sauter, B. Merkel, Testing the suitability of  
621 zerovalent iron materials for reactive walls. Environ. Chem. 2 (2005), 71–76.
- 622 [71] E.M. Pierce, D.M. Wellman, A.M. Lodge, E.A. Rodriguez, Experimental determination of  
623 the dissolution kinetics of zero-valent iron in the presence of organic complexants. Environ.  
624 Chem. 4 (2007), 260–270.
- 625 [72] C. Noubactep, On the operating mode of bimetallic systems for environmental remediation.  
626 J. Hazard. Mater. (2008), In Press, Available online 13 August 2008.

- 627 [73] R. Hernandez, M. Zappi, C. -H. Kuo, Chloride effect on TNT degradation by zerovalent iron  
628 or zinc during water treatment. *Environ. Sci. Technol.* 38 (2004), 5157–5163.
- 629 [74] J.S. Kim, P.J. Shea, J.E. Yang, J. -E. Kim, Halide salts accelerate degradation of high  
630 explosives by zerovalent iron. *Environ. Pollut.* 147 (2007), 634–641.
- 631 [75] D.R. Burris, T.J. Campbell, V.S. Manoranjan, Sorption of trichloroethylene and  
632 tetrachloroethylene in a batch reactive metallic iron-water system. *Environ. Sci. Technol.* 29  
633 (1995), 2850–2855.
- 634 [76] P.G. Tratnyek, M.M. Scherer, B. Deng, S. Hu, Effects of natural organic matter,  
635 anthropogenic surfactants, and model quinones on the reduction of contaminants by zero-  
636 valent iron. *Wat. Res.* 35 (2001), 4435–4443.
- 637 [77] P.D. Mackenzie, D.P. Horney, T.M. Sivavec, Mineral precipitation and porosity losses in  
638 granular iron columns. *J. Hazard. Mater.* 68 (1999), 1–17.
- 639 [78] J.A. Mielczarski, G.M. Atenas, E. Mielczarski, Role of iron surface oxidation layers in  
640 decomposition of azo-dye water pollutants in weak acidic solutions. *Applied Catalysis B:  
641 Environ.* 56 (2005), 289–303.
- 642 [79] D.H. Phillips, B. Gu, D.B. Watson, Y. Roh, L. Liang, S.Y. Lee, Performance evaluation of a  
643 zerovalent iron reactive barrier: Mineralogical characteristics. *Environ. Sci. Technol.* 34  
644 (2000), 4169–4176.
- 645 [80] K. Ritter, M.S. Odziemkowski, R.W. Gillham, An in situ study of the role of surface films  
646 on granular iron in the permeable iron wall technology. *J. Contam. Hydrol.* 55 (2002), 87 –  
647 111.
- 648 [81] M.M. Scherer, B.A. Balko, P.G. Tratnyek, The role of oxides in reduction reactions at the  
649 metal-water interface. *In Kinetics and Mechanism of Reactions at the Mineral/Water  
650 Interface*, Sparks, D.; Grundl, T., Eds; (1999) pp. 301–322.

651 [82] M.M. Scherer, K. Johnson, J.C Westall, P.G. Tratnyek, Mass transport effects on the  
652 kinetics of nitrobenzene reduction by iron metal. Environ. Sci. Technol. 35 (2001), 2804–  
653 2811.

654 [83] K.L. McGeough, R.M. Kalin, P. Myles, Carbon disulfide removal by zero valent iron.  
655 Environ. Sci. Technol. 41 (2007), 4607–4612.

656

657

657 **Table 1:** Main characteristics, iron content and percent methylene blue (MB) discoloration (P) of  
658 tested Fe<sup>0</sup> materials. MB removal were conducted in triplicates for 36 days under non-  
659 disturbed conditions. The material code (“code”) are from the author, the given form is  
660 as supplied; d (μm) is the diameter of the supplied material and the Fe content is given  
661 in % mass.

Supplier <sup>(a)</sup>	Supplier denotation	code	form	d (μm)	Fe (%)	P (%)
<b>MAZ, mbH</b>	Sorte 69 <sup>(b)</sup>	ZVI0	fillings	-	93 <sup>(c)</sup>	75 ± 2
<b>G. Maier GmbH</b>	FG 0000/0080	ZVI1	powder	≤ 80	92 <sup>(d)</sup>	88 ± 2
<b>G. Maier GmbH</b>	FG 0000/0200	ZVI2	powder	≤ 200	92 <sup>(d)</sup>	89 ± 1
<b>G. Maier GmbH</b>	FG 0000/0500	ZVI3	powder	≤ 500	92 <sup>(d)</sup>	88 ± 1
<b>G. Maier GmbH</b>	FG 0300/2000	ZVI4	fillings	200-2000	92 <sup>(d)</sup>	81 ± 4
<b>G. Maier GmbH</b>	FG 1000/3000	ZVI5	fillings	1000-3000	92 <sup>(d)</sup>	77 ± 4
<b>G. Maier GmbH</b>	FG 0350/1200	ZVI6	fillings	100-2000	92 <sup>(d)</sup>	88 ± 1
<b>Würth</b>	Hartgussstrahlmittel	ZVI7	spherical	1200	n.d. <sup>(e)</sup>	66 ± 1
<b>Hermens</b>	Hartgussgranulat	ZVI8	flat	1500	n.d.	67 ± 2
<b>G. Maier GmbH</b>	Graugussgranulat	ZVI9	chips		n.d.	71 ± 7
<b>ISPAT GmbH</b>	Schwammeisen	ZVI10	spherical	9000	n.d.	72 ± 6
<b>ConnellyGPM</b>	CC-1004	ZVI11	fillings		>96	76 ± 4
<b>ConnellyGPM</b>	CC-1190	ZVI12	fillings		>96	75 ± 9
<b>ConnellyGPM</b>	CC-1200	ZVI13	powder		>96	84 ± 1

662 <sup>(a)</sup>List of suppliers: MAZ (Metallaufbereitung Zwickau, Co) in Freiberg (Germany); Gotthart Maier  
663 Metallpulver GmbH (Rheinfelden, Germany), ISPAT GmbH, Hamburg (Germany), Connelly GPM Inc. (USA),  
664 <sup>(b)</sup>Scrapped iron material; <sup>(c)</sup> Mbudi et al. [52]; <sup>(d)</sup> average values from material supplier, <sup>(e)</sup>not determined.  
665

665

666 **Table 2:** Characteristics, surface coverage and function of the individual reactive materials of this667 study. Apart from Fe<sup>0</sup> the given value of specific surface area (SSA) for are the minima668 of reported data. Apart from Fe<sub>2</sub>O<sub>3</sub> the pH at the point of zero charge (pH<sub>pzc</sub>) is lower

669 than the initial pH value. Therefore, MB adsorption onto the negatively charged

670 surfaces is favorable. The surface coverage is estimated using the method presented by

671 Jia et al. [47]. The total surface that can be covered by the amount of MB present in 22

672 mL of a 0.063 mM is S<sub>MB</sub> = 0.997 m<sup>2</sup>.

673

System	pH <sub>pzc</sub>	SSA (m <sup>2</sup> g <sup>-1</sup> )	S <sub>available</sub> (m <sup>2</sup> )	Coverage (1)	Function
Fe <sup>0</sup>	7.6 <sup>a</sup>	0.29	0.032	31.3	MB reductant?
Fe <sup>0</sup> + MnO <sub>2</sub>	-	-	4.432	0.2	-
MnO <sub>2</sub>	2.0 - 6.0 <sup>b</sup>	40	4.4	0.2	delays CP availability
Fe <sub>2</sub> O <sub>3</sub>	7.5 - 8.8 <sup>c</sup>	60	6.6	0.2	mimics aged CP
Fe <sub>3</sub> O <sub>4</sub>	6.8 <sup>d</sup>	40	4.4	0.2	mimics aged CP
GAC	7.0 - 8.0 <sup>e</sup>	200	22	0.1	MB adsorbent
Fe <sup>0</sup> + GAC	-	(-)	22.032	0.1	-

674 <sup>a</sup>ref. [48], <sup>b</sup>ref [39], <sup>c</sup>ref. [49], <sup>d</sup>ref. [50], <sup>e</sup>ref. [51].

675

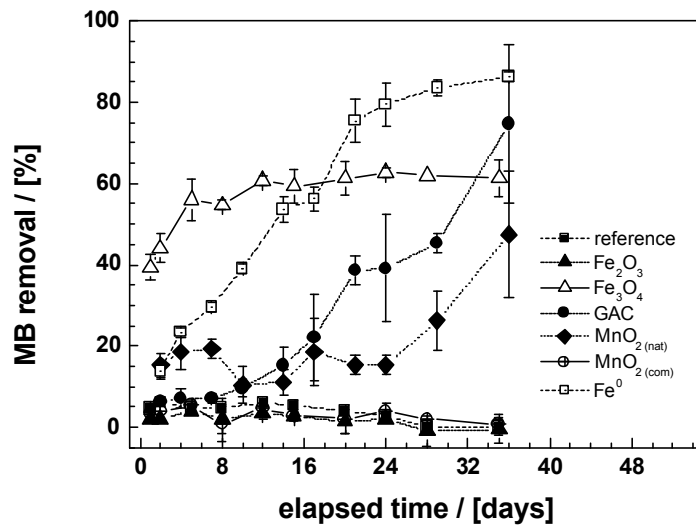
676

677



677 **Figure 1**

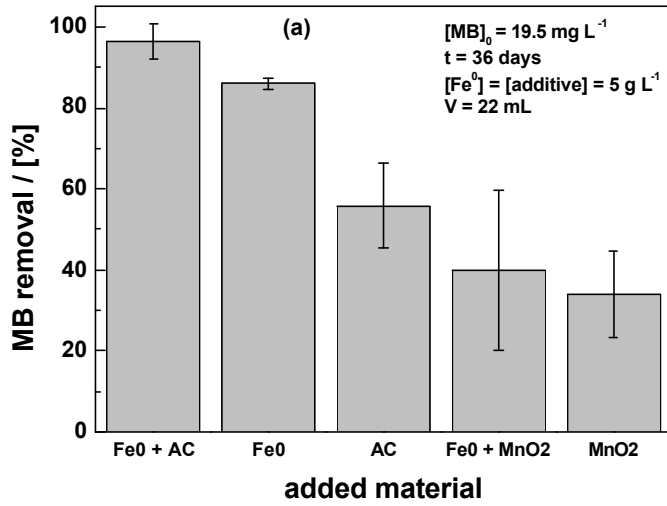
678



679

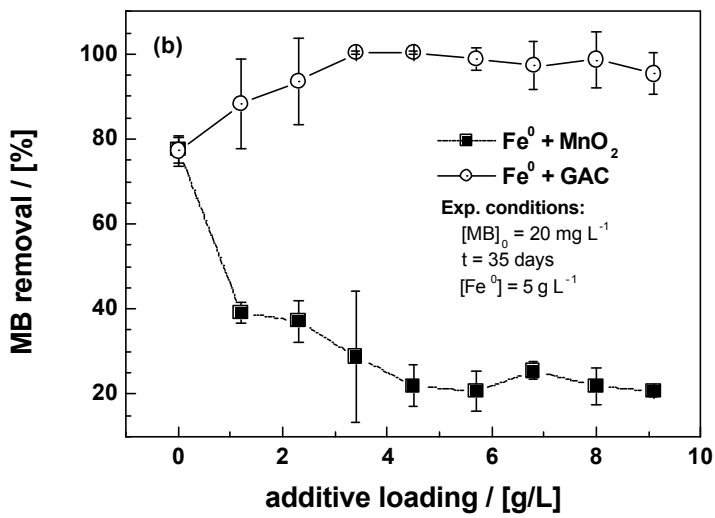
680

680 Figure 2



681

682



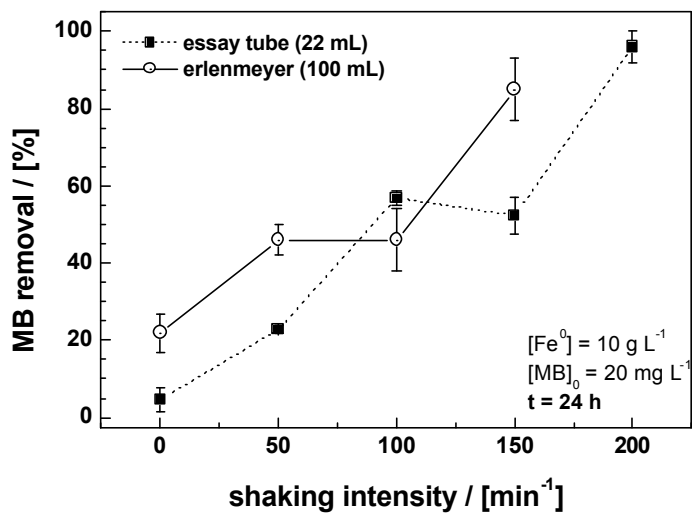
683

684

685

685 **Figure 3**

686



687

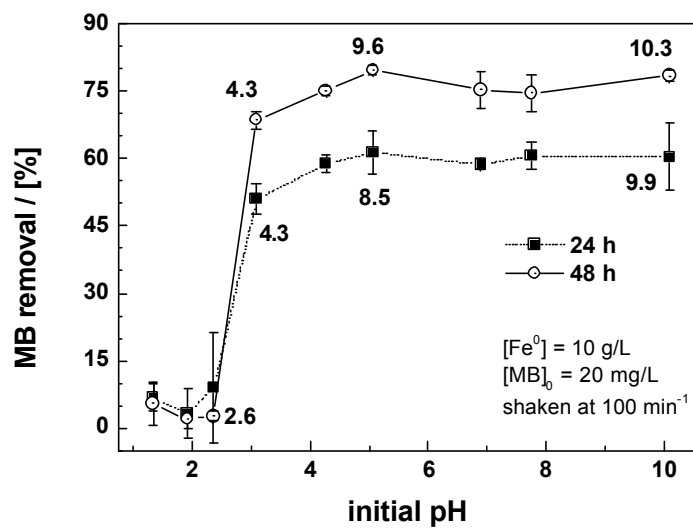
688

689

690

690 **Figure 4**

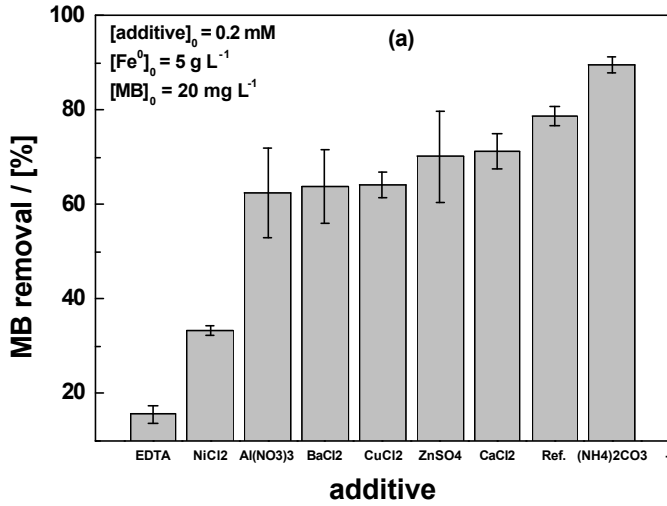
691



692

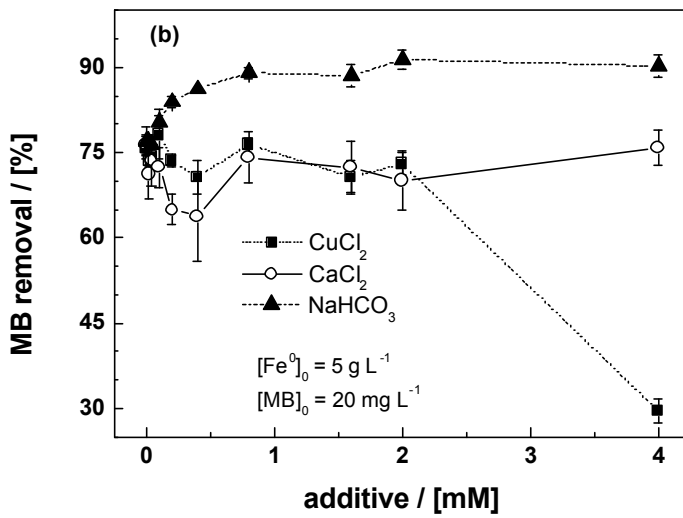
693

693 Figure 5



694

695



696

697

697 **Figure Captions**

698 **Figure 1:**

699 Methylene blue removal (%) as a function of equilibration time for the six tested reactive  
700 materials. The reference system is a blank experiment without additives. Two sets of experiments  
701 with  $\text{MnO}_2$  were conducted (see the text). The experiments were conducted in triplicate. Error  
702 bars give standard deviations. The lines are not fitting functions, they simply connect points to  
703 facilitate visualization.

704 **Figure 2:**

705 Methylene blue (MB) discoloration by metallic iron ( $\text{Fe}^0$ ), granular activated carbon (AC),  
706 manganese nodule ( $\text{MnO}_2$ ), and the mixtures “ $\text{Fe}^0 + \text{AC}$ ” and “ $\text{Fe}^0 + \text{MnO}_2$ ”. (a) extent of MB  
707 discoloration after 36 days, and (b) dependence of the MB discoloration on the additive loading  
708 for 35 days. The experiments were conducted in triplicate. Error bars give standard deviations.  
709 The lines are given to facilitate visualization.

710 **Figure 3:**

711 Effect of the mixing intensity ( $\text{min}^{-1}$ ) on discoloration of MB at initial pH 7.8. The system is  
712 mixed on a rotary shaker. The experiments were conducted in triplicate. Error bars give standard  
713 deviations. The lines simply connect points to facilitate visualization.

714 **Figure 4:**

715 Effect of initial pH on discoloration of MB by  $\text{Fe}^0$  for 24 and 48 h respectively. The experiments  
716 were conducted in triplicate. The reported numbers on the plots are the corresponding final pH  
717 values. Error bars give standard deviations. The lines simply connect points to facilitate  
718 visualization.

719 **Figure 5:**

720 Effect of solution chemistry on MB discoloration by metallic iron ( $\text{Fe}^0$ ): (a) extent of MB  
721 discoloration after 36 days for all tested additives, and (b) dependence of the MB discoloration on  
722 selected additive concentrations for 35 days. Ref. in figure “a” refers to the experiment in tap  
723 water (“no additive”). The experiments were conducted in triplicate. Error bars give standard  
724 deviations. The lines simply connect points to facilitate visualization.